COMMISSARIAT A L'ENERGIE ATOMIQUE

ELECTRICITE DE FRANCE

MODELING OF TWO-PHASE FLOW WITH THERMAL AND MECHANICAL NON-EQUILIBRIUM

by

G. HOUDAYER(1), G. LE COQ(3), B. PINET(1)
M. REOCREUX(2), J.C. ROUSSEAU(4)

(1) Electricité de France
Service Etudes et Projets Thermiques et Nucléaires

(2) Commissariat à l'Energie Atomique
Institut de Protection et de Sûreté Nucléaire (CEN-Fontenay-aux-Roses)

(3) Commissariat à l'Energie Atomique
Service d'Etudes de Réacteurs et de Mathématiques Appliquées (CEN-Saclay)

(4) Commissariat à l'Energie Atomique
Service des Transferts Thermiques (CEN-Grenoble)

5. Annual Water reactor safety research
information meeting. Washington, D.C. (USA)
1977, 7-11 november

CEA-CONF-4291

ABSTRACT

To improve two-phase flow modeling by taking into account thermal and mechanical non-equilibrium a joint effort on analytical experiment and physical modeling has been undertaken. A model describing thermal non-equilibrium effects is first presented. A correlation of mass transfer has been developed using steam water critical flow tests. This model has been used to predict in a satisfactory manner blowdown tests. It has been incorporated in CLYSTERE system code. To take into account mechanical non-equilibrium, a six equations model is written. To get information on the momentum transfers special nitrogen-water tests have been undertaken. The first results of these studies are presented.

CONTENT

NOMENCLATURE

A	Cross-section area
$\mathscr{C}$	Contour
g_z	Projection on z axis of the gravity acceleration
h	Specific enthalpy
I	Global momentum transfer (see paragraph 2.2)
$\vec{j}$	Heat flux density
$\vec{n}$	Unit vector on Oz
$\vec{n}_v$	Unit vector perpendicular to the interface
$\vec{n}_\ell$	Unit vector perpendicular to the interface
p	Pressure
Q	Global energy transfer (see paragraph 2.2)
t	Time
$\vec{V}$	Velocity
w	Projection on Oz of velocity
x	Quality
z	Abscissa
α_k	Volumetric fraction of phase k
Γ	Mass transfer term (see paragraph 2.2)
θ	Relaxation time
Φ	Contour heat transfer term
λ	Characteristic direction
ρ	Density
Σ	Surface
τ	Friction pressure drop
$\bar{\bar{\tau}}$	Deviatoric stress tensor

Subscripts

C	Related to contour
I	Related to the interface
k	Related to phase k
ℓ	Related to the liquid phase
m	Related to the mixture
sat	On the saturation line
v	Related to the vapor

0. INTRODUCTION

Numerous studies have been undertaken in many laboratories to get a better description of what really could happen during a Loss of Coolant Accident. Codes of the first generation (RELAP ...) give a quite good prediction and can be used in any case in a conservative form. However in order to obtain an evaluation of the safety margins, advanced codes are being developed. The objective of these codes is to get the most realistic description. In these tentatives some encouraging results have been obtained but many problems are not yet completely solved as for example the downcomer and pump modeling, the reflood prediction, stratification in case of small break, steam water mixing prediction.

In all these problems a common point is the two-phase flow modeling with the necessity of taking into account thermal and mechanical non-equilibrium. To improve this modeling, a joint effort on analytical experiment and on physical modeling has been undertaken. The physical models are developed from the analysis of the experimental results and in a reverse approach, experiments are performed to obtain answers to questions raised by the physical modeling.

In the first part, results on thermal non-equilibrium modeling are presented. These results have led to the CLYSTERE code. As this thermal non-equilibrium modeling is not sufficient and as mechanical non-equilibrium has to be taken into account, a model have been written and special modeling experiments have been undertaken. The first results of these studies are presented in the second part of this paper.

1. THERMAL NON-EQUILIBRIUM

1.1 Steam-water flows : MOBY DICK experiment

The experimental results which have been used first for the thermal non-equilibrium analysis are the first series of critical flow tests in steam-water mixtures performed on the MOBY DICK loop. As these tests have been already extensively described [REOCREUX, 1974], [GUIZOUARN, PINET and al, 1975], [REOCREUX, 1976] only the main results will be recalled here.

The test section is positionned vertically and consists of a lower part of constant 20 mm or 14 mm inner diameter, about 2.3 m long followed by a 327 mm long, 7 degrees straight diffuser ending in a constant diameter part. The inlet flow is subcooled and steam-water flow develops in the test section by flashing. The investigated range of parameters is 1.5 to 7.0 bars for the pressure at the throat, qualities less than 0.01 and flowrates from 4000 kg/m^2.s to 15000 kg/m^2.s.

Examples of results are given in Figure 1 where axial pressure profiles along the whole test section are given and in Figure 2 where axial pressure profiles and void fraction profiles upstream and downstream of the throat are given in a larger size.

In these tests the location of the onset of vaporization (abscissa Z_{eb} in Figures 1 and 2) can be determined by the pressure line and the void fraction profile. At this point the liquid appears to be superheated and the superheat can be evaluated from the difference between the pressure P_{eb} and the local saturation pressure P_{sat} (T_E) (Fig. 1, 2). In the conditions of our tests the superheat varies from 2 to 3°C. The distance Z_{eb}-Z_{sat} (Fig. 1) enables the calculation of the vaporization delay time which varies here from 0.1 to 0.2 second.

Assuming a slip ratio and a vapor temperature, the liquid temperature can be calculated from the measured void and pressure profiles. In Figure 3 some profiles are given of the saturation temperature T_{sat} and of the liquid temperature T_L compared to the inlet temperature T_E. One can see in the left column of Figure 3 that the superheat of the liquid increases from the onset of vaporization to the throat where liquid superheat of 4°C to 5°C can be reached. When the flow rate increases the variation of the liquid temperature becomes smaller and reaches only a few tenths of degrees C at the highest flow rate.

On the right column are given the results of tests performed with a grid placed upstream of the throat. A similar behaviour can be observed with lower non-equilibrium level due to the cavitation in the grid.

The results presented in Figure 3 are computed with the vapor at saturation temperature. Deviations from saturation do not affect the results significantly. The slip ratio is taken equal to 1. Higher slip ratios give lower liquid temperatures. At low flow rates deviations of 1°C can be observed for a slip ratio of 3. At high flow rates the deviations of the liquid temperature due to slip variations do not affect significantly the large increase of the non-equilibrium.

Among all the conclusions which can be drawn from these tests, it appears that thermal non-equilibrium is here one of the most important phenomena. We have here experimental information on how a two phase mixture which is initially superheated or not (tests without or with a grid) behaves when it is submitted to a steep variation of pressure. The way the thermal non-equilibrium increases and then reduces gives experimental information on the dynamics of vaporization and it is this information which is used in our attempt of thermal non-equilibrium modeling.

1.2 Modeling

As in the considered phenomena the mechanical non-equilibrium seems not to be the main effect, the slip ratio is in a first approach assumed equal to 1. The analysis of the results shows that the thermodynamic state of the fluid at a given point depends on the past behaviour of the fluid along the flow and not only on the local fluid parameters. The thermal non-equilibrium has then to be the solution of some differential equation describing the flow behaviour (instead of being given by a correlation).

The set of equations is derived from the conservation laws. It consists (see Table 1) of the mass, momentum and energy balance for the mixture and of the vapor mass balance. These four equations are included in the code SERINGUE / BAUER, HOUDAYER, SUREAU, 1976 /.

To solve this set of equations we need an expression for the mass transfer Γ. Assuming a friction law at the wall, values of the mass transfer can be deduced from the measured pressure lines in the MOBY DICK experiments. These values can be determined with a good approximation because the acceleration pressure drops are preponderant and therefore the obtained values are not very sensitive to the friction laws.

We have then at each point and in all the tests (without and with a grid) the values of the mass transfer Γ. The combination of the mixture mass balance and of the vapor mass balance can be written :

$$\frac{Dx}{Dt} = \frac{\Gamma}{\rho_m}$$

Using the concept of first order relaxation processes, Γ is written in the following form :

$$\frac{\Gamma}{\rho_m} = \frac{x^* - x}{\theta}$$

where x^* is the equilibrium quality and θ a relaxation time.

From the calculated values of Γ a correlation of θ has been developed. The obtained expression is :

$$\theta = \frac{660}{p^{0.515}\ \alpha_v^{0.954}\ V_m^{1.89}} \approx \frac{1.5}{\alpha_v\ V_m^2} \qquad (1)$$

Comparisons of experimental and correlated values are given in Figure 4.

1.3 Results

1.3.1 Recalculation of MOBY DICK tests

The expression (1) of Γ has been used in the code SERINGUE to recalculate the MOBY DICK tests. The correlation (1) is completed for

very low void fractions by the correlation :

$$\theta = \frac{2.7\ 10^{-5}}{x^{*2}} \qquad (2)$$

which is used to describe the germination process.

Results are given in Figure 5. The agreement between the calculated and the measured pressure lines is good especially upstream of the throat. .

For given inlet conditions (pressure and temperature) the calculated flow rates are maximum. However the sound velocity of the model is not reached at the throat. The calculated flow rates are given in table 2. Discrepancies with experimental values of 10% to 20% can be observed.

Although the Γ law is adjusted on the experiment itself, these relatively good recalculations show that no deviation due to eventual accumulated errors is obtained.

1.3.2 Prediction of CANON tests

CANON tests have been predicted by the code SERINGUE and by the code BERTHA [ROUSSEAU, 1975] .

The code BERTHA uses a non-equilibrium equation based on enthalpy variation instead of a vapor mass balance. But it has been shown that the two set of equations are practically "equivalent". The code BERTHA uses the method of characteristics whereas the code SERINGUE uses an implicit method.

CANON experiment (figure 6) consists of a 4 m long, 0.10 m inner diameter horizontal tube. It is filled with water with a pressure of 32 bars and a temperature of 220°C. A bursting device allows the opening of a full sized break at one end of the tube in a very short time (10^{-7} s).

In Figure 7 are given the results obtained with BERTHA at 3.10^{-3} second with the same law for Γ as before (formula (1) and (2)). One can notice the steep gradient obtained near the exit. This implies the necessity for a model to take into account thermal non-equilibrium in this zone. On a numerical point of view, a very small mesh size (about 1 mm) has to be used near the break.

In Figure 8 is given the comparison of the calculated void fraction with the average void fraction in a cross-section measured by a neutron diffusion technique. In Figure 9 is given the comparison of the calculated and measured pressures in the same cross-section as in Figure 8. Good agreement is obtained.

It has to be emphasized that no special adjustments have been made in SERINGUE and BERTHA code to predict CANON test. The Γ law is the one which has been adjusted on the MOBY DICK experiment and no contraction coefficient is used at the break. This is justified by the fact that the range of parameters are similar in the two experiments.

1.3.3 Prediction of SUPER CANON tests

SUPER CANON is an experimental apparatus of similar geometry to CANON. The initial conditions are different : the pressure is 150 bars and the temperature of the water is 300°C. A diaphragm of 50 mm inner diameter is positionned just upstream of the break.

A comparison between measured and calculated pressures is given in Figure 10. The same codes and the same mass transfer law as before have been used. The agreement between measured and calculated pressure is not good. This can be explained by the necessity of improvement of the correlation Θ at higher pressures than the pressures for which it has been adjusted (1 to 10 bars).

A new experiment SUPER MOBY DICK is designed for that purpose. This loop will be similar to MOBY DICK, but the explored range of parameters will be :

- inner diameter of the test section : 14 mm or 20 mm (as in MOBY DICK)
- pressure : 10 to 100 bars
- flow rate up to 20 kg/s.

Detailed pressure lines and void fraction profiles using the γ-attenuation technique, will be measured as it is done in MOBY DICK.

This experiment will give us experimental information to validate the mass transfer law at high pressures. However, the experiments which are used are small scale experiments (14 mm and 20 mm diameter in MOBY DICK, 100 mm diameter in CANON). Therefore this model has to be verified for larger scale experiments. This will be done with MARVIKEN-CFT experiment.

1.4 CLYSTERE Code

This flow model is incorporated in the CLYSTERE system code which simulates the primary circuit of a PWR during a LOCA / SUREAU, HOUDAYER, 1975 /, / BAUER, HOUDAYER, SUREAU, 1976 /.

An axial representation is used (Figure 11). The core is simulated by four parallel channels ; cross-flows between two of them are taken into account. Oxidation, swelling and rupture of the clad are simulated. The pump model is an axial model / GRISON, 1977 / based on the same flow modeling.

At present we are testing CLYSTERE. Examples of results are given in Figures 12 and 13. In Figure 12 are given the pressure lines in all the reactor components at 0.01 second. In Figure 13 are given the same pressure lines at 0.04 second.

These Figures show how the pressure waves propagate in the circuit and how flashing initiates in the different components. We can notice that inside the pump flashing occurs before the inlet and outlet pressures have reached the saturation pressure.

The CLYSTERE code is difficult to use due to the large computing time and the rigidity of its organization. Furthermore the validity of the flow model is limited as it does not take into account mechanical non-equilibrium. To improve these points new studies have been undertaken.

2. MECHANICAL NON-EQUILIBRIUM

2.1 Short comings of the SERINGUE model

During the first seconds of the blowdown and as the first calculations made with CLYSTERE show, the thermal non-equilibrium seems to be the key effect at the beginning of flashing. After these first seconds the mechanical non-equilibrium cannot be neglected and in the parts where thermal equilibrium is almost reached, it can be the predominant effect.

Mechanical non-equilibrium has to be taken into account for example in reflood calculations where it controls the behaviour of the water entrainment. A second example is steam water mixing where the differences of velocities between the steam and the water injected can be very high. In the case of small breaks it is certainly one of the predominant phenomena.

Some experimental results cannot be predicted without introducing mechanical non-equilibrium. In MOBY DICK test calculations (see Figure 5) the calculated pressure lines presents a too large protuberance after the throat. This cannot be avoided without slip. In the OMEGA experiment the adiabatic blowdown of a test section placed between two vessels does not give the same depressurization rate if the break is placed in the upper or lower vessel. As this apparatus is strictly symetrical, this cannot be explained if slip effects leading to stratifications are not taken into account.

2.2 Mechanical non-equilibrium modeling

Different steps in the way of taking into account mechanical non-equilibrium can be distinguished.

The first way which is widely used with some success consists of developing correlations for the difference between the averaged

velocities of each phase or between the velocity of one phase and some mixture velocity as in the drift flux model. These correlations are functions of the other parameters of the fluid and are adjusted by using steady-state experiments. One important question which arises from this type of modeling is the validity for transient two-phase flow of such correlations which has been adjusted in steady state, specially when the transient is "fast".

The next step is what is called the two-fluid modeling. Instead of describing the mechanical non-equilibrium by some relation between the velocities, expressions of transfers between phases are developed. Since the evolution of the mixture is a consequence of the transfers at the wall and at the interfaces, it seems more rational to derive transfer laws than to derive evolution laws. The transfer laws must be adjusted on steady state experiments in the same way which is used for the evolution laws. But as we try to describe directly the physical causes i.e. the transfers, we can hope that the model which is adjusted in steady state works in transient conditions.

However these transfer laws are generally correlated as functions of the flow parameters. It has been shown that rapid transients like wave propagations are not well described [REOCREUX, 1974] [BOURE, GIOT, FRITTE, REOCREUX, 1976]. The further step is then to include derivative terms in the transfer laws so that the influence of the transient conditions on the transfers can be in some way taken into account.

It appears finally desirable to write two momentum equations in order to analyse the dynamics of mechanical non-equilibrium. It has to be emphasized that this is similar to the technique now very often used for describing thermal non-equilibrium : two continuity equations are written which allows the correlation of mass transfer laws instead of some non-equilibrium evolution.

The complete model of two-phase flow will then include two continuity and two momentum equations. In order to avoid some assumptions on the thermodynamical state of one phase and as this seems not to change drastically the dynamic behaviour of the system of equations [FRITTE, 975], two energy equations will be used leading to a six equations model.

These six equations have been already derived [VERNIER, DELHAYE, 1968], [BOURE, REOCREUX, 1972], [BOURE and al, 1976], [ISHII, 1975]. They are given in table 3. They are obtained by averaging statistically and in a cross-section the local and instantaneous conservation equations derived from the conservation laws. Assumptions and conventions are made to obtain a useable set of equations (see [BOURE, REOCREUX, 1972], [REOCREUX, 1974]).

In the right-hand side members of table 3 appear the transfer terms :

$$\Gamma = -\frac{1}{A}\overline{\oint_{\mathcal{J}} \rho_V \, (\vec{V}_V - \vec{V}_I) \, \vec{n}_V \, \frac{d\Sigma}{dz}}$$

which is the mass transfer term between the phases.

$$I = -\frac{1}{A}\left[\overline{\oint_{\mathcal{J}} \rho_V \left[(\vec{V}_V - \vec{V}_I) \, \vec{n}_V\right] \vec{V}_V \, \frac{d\Sigma}{dz}}\right]_z + \frac{1}{A}\left[\overline{\oint_{\mathcal{J}} \bar{\tau}_V \, \vec{n}_V \, \frac{d\Sigma}{dz}}\right]_z$$

which is the global momentum transfer term. The first term is the momentum transferred to the vapour resulting from the mass transfer. The second term are the viscous stresses acting on the vapour.

$$Q = -\frac{1}{A}\overline{\oint_{\mathcal{J}} \rho_V \left(h_V + \frac{\vec{V}_V^2}{2}\right) (\vec{V}_V - \vec{V}_I) \, \vec{n}_V \, \frac{d\Sigma}{dz}} + \frac{1}{A}\overline{\oint_{\mathcal{J}} (\bar{\tau}_V \cdot \vec{n}_V) \, \vec{V}_V \, \frac{d\Sigma}{dz}} - \frac{1}{A}\overline{\oint_{\mathcal{J}} \vec{J}_V \cdot \vec{n}_V \, \frac{d\Sigma}{dz}}$$

which is the global energy transfer term. The first term is the enthalpy and kinetic energy transferred to the vapour resulting from the mass transfer. The second term is the energetic contribution of the friction at the interfaces. The third term is the energy transferred as heat.

2.3 Modeling experiment

To use the six equations model we need experimental information on the mass, momentum and energy transfers. It is then necessary to separate the thermal non-equilibrium effects and the mechanical non-equilibrium effects. This can be achieved by considering two-component flows whithout mass transfer.

For these reasons, series of tests with nitrogen-water mixtures have been undertaken on the MOBY DICK loop. The same test-section as during the steam-water tests is used (14 mm inner diameter). This eliminates geometry effects in the comparison of thermal and mechanical non-equilibrium. The nitrogen is injected 98 cm upstream of the throat (Figure 14). Qualities cannot exceed 0.2%. The range of temperature can vary from 20 to 70°C.

In nitrogen-water flow the mass transfer is practically zero and the remaining transfers are the momentum and heat transfer. It is probable that the heat transfer is sufficient to obtain equal temperature of the phases. Nevertheless a device has been realised so that different nitrogen and water temperatures can be obtained at the injection

point. A comparison with isothermal injection will give an idea of the heat transfer term. Furthermore, as water temperature variations induce in the considered range large viscosity variations, it will give information on the influence of viscosity on momentum transfers. It will also allow better extrapolation to higher temperatures.

Examples of results are given in Figure 15. A steep pressure decrease can be observed near the throat when the critical conditions are obtained. Therefore the analysis of the results will give information on the dynamics of momentum transfer and thus on the mechanical non-equilibrium.

A first qualitative comparison with the steam-water tests in the same geometry shows that the gradients at the throat are steeper in the nitrogen-water tests and that the pressure recovery in the diffuser presents significant differences of behaviour.

2.4 Preliminary results

2.4.1 Transfer laws

Tentative forms of these laws are written by using the concept of reducing the non-equilibrium by first order relaxation processes.

The mass transfer law is taken in a similar form than in the 4 equations model :

$$\Gamma = \rho_m \frac{x^* - x}{\theta_1}$$

The momentum transferred to the vapour resulting from the mass transfer is written ΓV_1, where V_1 is an average velocity on the interface. A first evaluation of the velocity V_1 is given by :

$$V_1 = (1-x)\, w_v + x\, w_\ell$$

The global momentum transfer is then written :

$$I = \Gamma V_1 - \rho_m\, x\, (1-x)\, \frac{w_v - w_\ell}{\theta_2}$$

The enthalpy and kinetic energy transferred to the vapour resulting from the mass transfer is written ΓH_T, where H_T is an average total enthalpy on the interface. This average total enthalpy is evaluated by :

$$H_T = \frac{1}{xC_{pv} + (1-x)C_{p\ell}} \left[(1-x)C_{p\ell}\left(h_v + \frac{w_v^2}{2}\right) + xC_{pv}\left(h_\ell + \frac{w_\ell^2}{2}\right) \right]$$

The energetic contribution of the friction is evaluated by :

$$(I - \Gamma V_1)\ V_2$$

where V_2 is an average velocity on the interface evaluated by

$$V_2 = (1-x)C_{p\ell} w_v + x C_{pv} w_\ell$$

The total energy transfer is then written :

$$Q = \Gamma H_T + (I-\Gamma V_1)\ V_2 \quad - \rho_m \frac{x(1-x)\ C_{pv}\ C_{p\ell}}{x\ C_{pv} + (1-x)\ C_{p\ell}} \frac{\left[T_v - T_\ell\right]}{\theta_3}$$

2.4.2 Mechanical non-equilibrium analysis using MOBY DICK tests with nitrogen-water mixture

MOBY DICK tests are analysed with the six equations model. For these tests :

- Γ is taken equal to zero
- the relaxation time θ_3 is taken sufficiently small so that the two phases are at the same temperature
- for each phase the friction at the wall is written :

$$A\tau_{KC} = f\ \alpha_k\ p_w \rho_k\ w_k\ |w_k|$$

From the measured pressure lines it is possible with the model to calculate at each point of the flow, the flow parameters and the momentum transfer I. From these calculated values of I, correlations of θ_2 are developed.

An example of prediction of the test 2069 using a preliminary correlation of θ_2 is given in Figure 16. The maximum flow rate is predicted with a 8 % error.

This study is now under progress. The first tentative of analysis has shown experimental needs :

- To start the calculation of the momentum transfer I from the pressure lines, accurate inlet conditions are needed.
  The quality is known by the separate nitrogen and water flow rates measurements. To obtain the average void fraction in a cross section, measurements by X-ray attenuation of the void profiles in a cross-section have been developed. In the new series of tests the knowledge of the quality and of the void fraction allows the calculation of the inlet velocities of each phase.

- To develop correlations a large range of parameters specially for void and pressure is needed. A corresponding, experimental program is under taken.

2.4.3 Characteric directions. Application to flow rate reversal and counter-current flow

It is known that the six equations model with algebraic transfer laws has, in the pratical range of parameters, two complex characteristic directions [BOURE, 1973]. Difficulties in the definition of the boundary conditions specially in flow rate reversal and counter-current flow can be expected. To clarify these problems the conditions on the transfer laws so that an hyperbolic set of equations is obtained are being studied.

To change the nature of the characteristic directions we have to change the left hand side members, that is the transfer terms have to include derivative terms. By these derivative terms we change the dynamic coupling between the phases [BOURE, REOCREUX, 1972], [REOCREUX, 1974]. As the complex characteristics appear in models with unequal velocities and specially when two phasic momentum equations are used, it seems that the coupling between the phases by momentum transfer has to be incriminated.

For these reasons a derivative term is introduced in the momentum transfer. This term has the following form :

$$- A\beta \rho_3 \alpha_v \alpha_\ell \left[\frac{\partial}{\partial t} (w_v - w_\ell) + W_3 \frac{\partial}{\partial z} (w_v - w_\ell) \right]$$

β, ρ_3 and W_3 are adjustable parameters.

This form comes from physical considerations on induced mass effects [MECREDY, HAMILTON, 1972] [P.S. ANDERSEN, 1977]. Till now few parametric studies have been done on this derivative term.

In Figure 17 are given, as example in the case of counter-current flow, the areas for W_3, where the six characteristic directions are real.

In Figure 18 is given the effect on the sound velocity : $\beta = 0$ corresponds to the six equations model ; $\beta = \infty$ give a sound velocity close to the one of the frozen model. Infinite values of β seems then to give a coupling between phases similar to the one assumed by the equal velocity assumption. The differences can be explained by the fact that no coupling by the energy transfer is taken into account in the present model contrarily as it is in the frozen model.

Taking W_3 at the boundary of the real and complex regions and with a value for β of 0.75, the evolution of the characteristics λ_i along the flow for a nitrogen-water test have been calculated and are given in Figure 19. It can be seen that the characteristic λ_4 cancels at the throat.

3. CONCLUSION

Based on steam-water experiments performed on the MOBY DICK loop a model describing thermal non-equilibrium effects have been developed. This model has been used to recalculate the experiment and to predict CANON test. A good agreement has been obtained. This model has been incorporated in the reactor code CLYSTERE.

This modeling is not sufficient and mechanical non-equilibrium has to be considered. To improve this modeling, a six equations model have been written. In order to develop the transfer laws, nitrogen-water tests are being performed. It allows the separation of mechanical non-equilibrium effects from mixed thermal and mechanical ones.

Other studies are under progress on possible forms of the transfer laws. One study refers to the use of the second principle of thermodynamics. Within the limits of the linear thermodynamics, the total entropy variation of the mixture can be written proportionally to the differences of temperatures, gibbs potentials and velocities of each phase. The mass, momentum and energy transfers can then be divided into reversible and irreversible transfers. The irreversible part can be expressed in function of the previous differences.

From the first results, new series of tests have been undertaken to answer to some needs of the modeling. These first results have to be improved and then extended in all range of parameter. Experiments (SUPER MOBY DICK, SUPER CANON) have already been planned for this purpose. The modeling studies are connected to numerical studies with the problem of the complex characteristic directions. Description of flow reversal and counter-current flow for example may need precisions on this problem.

At the same time flexible system computer code is being developed (POSEIDON) to incorporate this modeling and others (eventual different flow models, conduction model, fuel model...).

REFERENCES

ANDERSEN, P.S.
The two-Fluid Test Code, RISQUE
First Progress Report NORMAV-D-036 (February 1977)

BAUER, E.G. ; HOUDAYER, G.R. ; SUREAU, H.M.
A Non-Equilibrium Axial Flow Model and Application to loss of Coolant Accident Analysis ; the CLYSTERE system code.
Specialists Meeting on Transient Two-Phase Flow, Toronto (1976)

BOURE, J.A. ; REOCREUX, M.
General Equations of Two-Phase Flows. Applications to Critical Flows and to Non-Steady Flows
Fourth all-union heat transfer Conference (Minsk, 1972)

BOURE, J.A.
Dynamique des Ecoulements Diphasiques : propagation de petites perturbations
Rapport CEA-R-4456 (1973)

BOURE, J.A. ; FRITTE, A. ; GIOT, M.M. ; REOCREUX, M.L.
Highlights of two-phase critical Flow
Int. J. Multiphase Flow Vol. 3, pp.1-22 (1976)

GRISON, P. ; LAURO, J.F.
Two-phase performance characteristics of a PWR primary pump under LOCA-conditions
Heat and Flow in water Reactor Safety Conference - Manchester (13-15 Sept. 1977)

GUIZOUARN, PINET, BARRIERE, PIETRI
Etude expérimentale des débits critiques en écoulement diphasique eau-vapeur à faible titre dans un canal avec divergent de 7° à des pressions au col de 2 à 7 bars
Note Interne STT n° 501 (1975)

ISHII, M.
Thermo-Fluid Dynamic Theory of Two-Phase Flow
Eyrolles - Paris, 1975

MECREDY, R.C. ; HAMILTON, L.S.
The effects of non-equilibrium heat and mass transfer in two-phase sound speed
Int. J. Heat and Mass Transfer Vol. 15, pp.61-72 (1972)

REOCREUX, M.L.
Contribution à l'étude des débits critiques en écoulement diphasique eau-vapeur
Thèse Université Scientifique et Médicale de Grenoble (1974)

REOCREUX, M.L.
Experimental Studies of Steam Water Chokad Flow
Specialists Meeting on Transient Two-phase Flow (Toronto, 1976)

ROUSSEAU, J.C. ; RIEGEL, B.
Blowdown Experiment on CANON ; Interpretation by the BERTHA code
European Two-Phase Flow Group Meeting, Haïfa (1975)

SUREAU, H.M. ; HOUDAYER, G.R.
Modélisation des écoulements eau-vapeur pour l'étude des accidents de perte de réfrigérant des chaudières nucléaires à eau ordinaire
Rapport EdF-SEPTEN TC 75-11 (TD 170) (1975)

VERNIER, P. ; DELHAYE, J.M.
General Two-Phase Flow Equations Applied to the Thermohydrodynamics of boiling nuclear reactors
Acta Technica Belgica, EPE IV, 1-2

TABLE 1

Mixture Mass balance

$$\frac{\partial}{\partial t} A\rho_m + \frac{\partial}{\partial z} A\rho_m V_m = 0$$

Mixture Momentum balance

$$\frac{\partial}{\partial t} A\rho_m V_m + \frac{\partial}{\partial z} A\rho_m V_m^2 + A \frac{\partial p}{\partial z} = - A \tau_c + A \rho_m g_z$$

Mixture Energy balance

$$\frac{\partial}{\partial t} A \rho_m (h_m + \frac{V_m^2}{2}) - A \frac{\partial p}{\partial t} + \frac{\partial}{\partial z} A \rho_m V_m (h_m + \frac{V_m^2}{2}) = A \phi_c + A \rho_m V_m g_z$$

Vapor Mass balance

$$\frac{\partial}{\partial t} A\alpha_v \rho_v + \frac{\partial}{\partial z} A \alpha_v \rho_v V_m = A \Gamma$$

$$\rho_m = \alpha_v \rho_v + \alpha_\ell \rho_\ell$$

$$V_m = w_v = w_\ell$$

$$h_m = \frac{1}{\rho_m} (\alpha_v \rho_v h_v + \alpha_\ell \rho_\ell h_\ell)$$

TABLE 2

Test n°	Measured flow rate kg/s	Calculated maximum flow rate kg/s	Error	Average error
403	1.318	1.152	12,6 %	13 %
426	1.37	1.115	18,6 %	
448	1.323	1.217	8 %	
400	2.05	1.283	37,4 %	24,8 %
442	2.01	1.763	12,3 %	
406	2.739	2.465	10 %	7,3 %
429	2.66	2.42	9 %	
451	2.677	2.597	2,9 %	
409	3.239	3.267	- 0,8 %	- 1,1 %
434	3.177	3.243	- 2,1 %	
456	3.214	3.200	- 0,4 %	

TABLE 3

Mass balance

$$\frac{\partial}{\partial t} A \alpha_v \rho_v + \frac{\partial}{\partial z} A \alpha_v \rho_v w_v = A \Gamma$$

$$\frac{\partial}{\partial t} A \alpha_\ell \rho_\ell + \frac{\partial}{\partial z} A \alpha_\ell \rho_\ell w_\ell = - A \Gamma$$

Momentum balance

$$\frac{\partial}{\partial t} A \alpha_v \rho_v w_v + \frac{\partial}{\partial z} A \alpha_v \rho_v w_v^2 + A \alpha_v \frac{\partial p}{\partial z} = AI - A\tau_{vc} + A \alpha_v \rho_v g_z$$

$$\frac{\partial}{\partial t} A \alpha_\ell \rho_\ell w_\ell + \frac{\partial}{\partial z} A \alpha_\ell \rho_\ell w_\ell^2 + A \alpha_\ell \frac{\partial p}{\partial z} = AI - A\tau_{\ell c} + A \alpha_\ell \rho_\ell g_z$$

Energy balance

$$\frac{\partial}{\partial t} A \alpha_v \rho_v \left(h_v + \frac{w_v^2}{2}\right) + \frac{\partial}{\partial z} A \alpha_v \rho_v w_v \left(h_v + \frac{w_v^2}{2}\right) - A \alpha_v \frac{\partial p}{\partial t} =$$

$$+ AQ + A \phi_{vc} + A \alpha_v \rho_v w_v g_z$$

$$\frac{\partial}{\partial t} A \alpha_\ell \rho_\ell \left(h_\ell + \frac{w_\ell^2}{2}\right) + \frac{\partial}{\partial z} A \alpha_\ell \rho_\ell w_\ell \left(h_\ell + \frac{w_\ell^2}{2}\right) - A \alpha_\ell \frac{\partial p}{\partial t} =$$

$$- AQ + A \phi_{\ell c} + A \alpha_\ell \rho_\ell w_\ell g_z$$

Notation

$$\tau_{vc} = - \frac{1}{A} \overline{\oint_{\mathcal{C}_v} \vec{\tau}_v \vec{n}_v \frac{d\xi}{dz}}$$

$$\phi_{vc} = - \frac{1}{A} \overline{\oint_{\mathcal{C}_v} \vec{J}_v \vec{n}_v \frac{d\Gamma}{dz}}$$

Γ, I and Q are defined in the text.

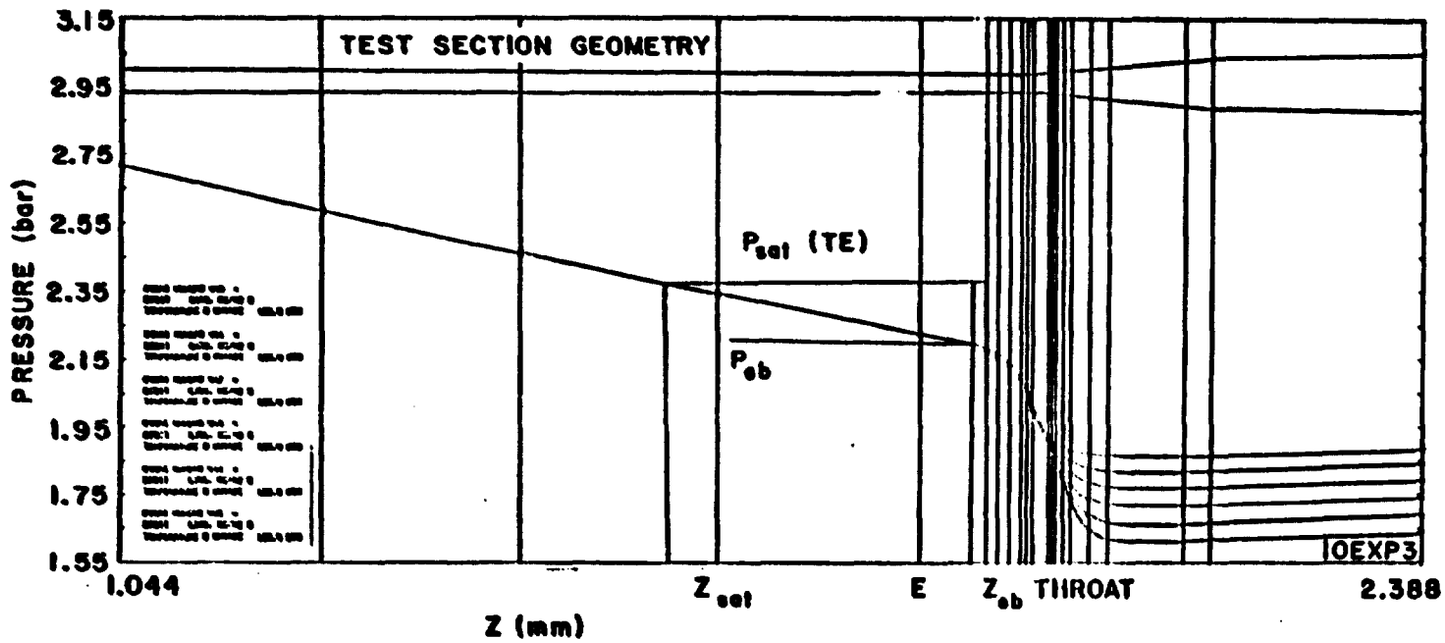

FIG. 1 - STEAM-WATER CRITICAL FLOW TESTS - PRESSURE LINES

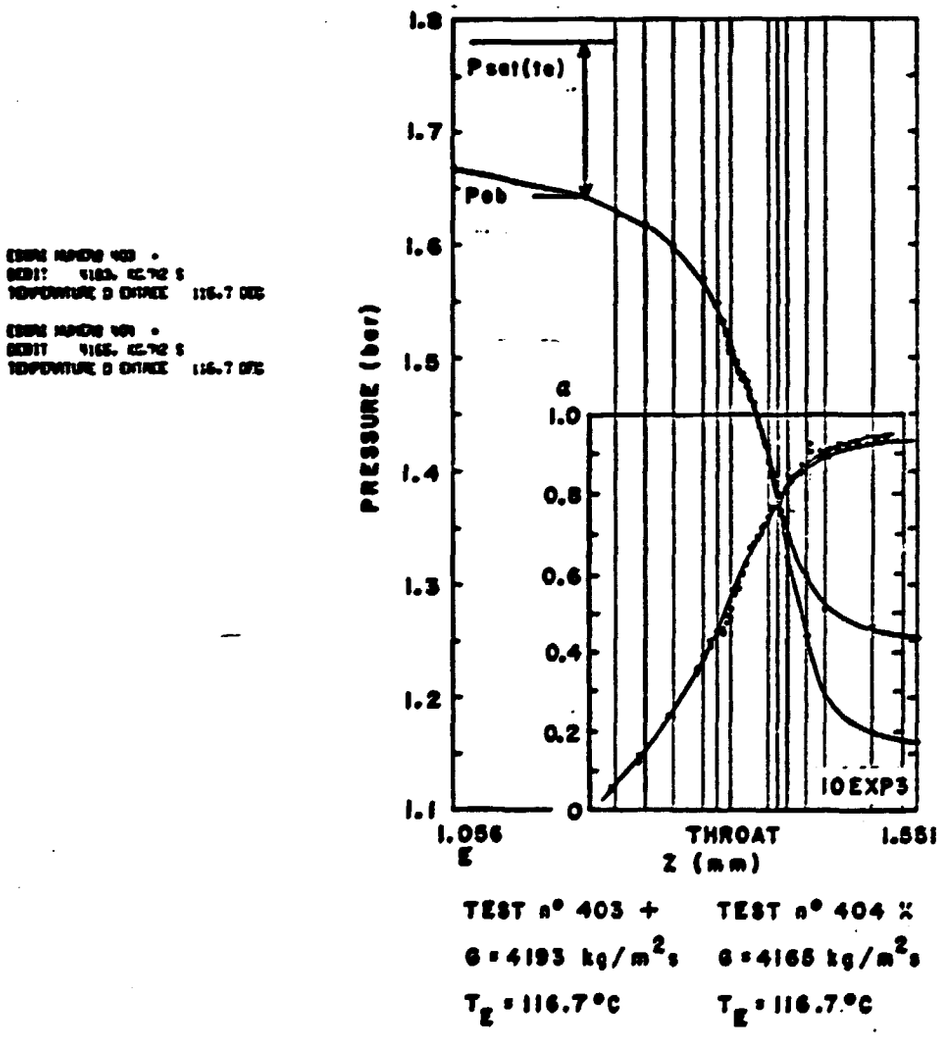

FIG. 2 STEAM WATER CRITICAL FLOW TESTS
PRESSURE AND VOID FRACTION LINES

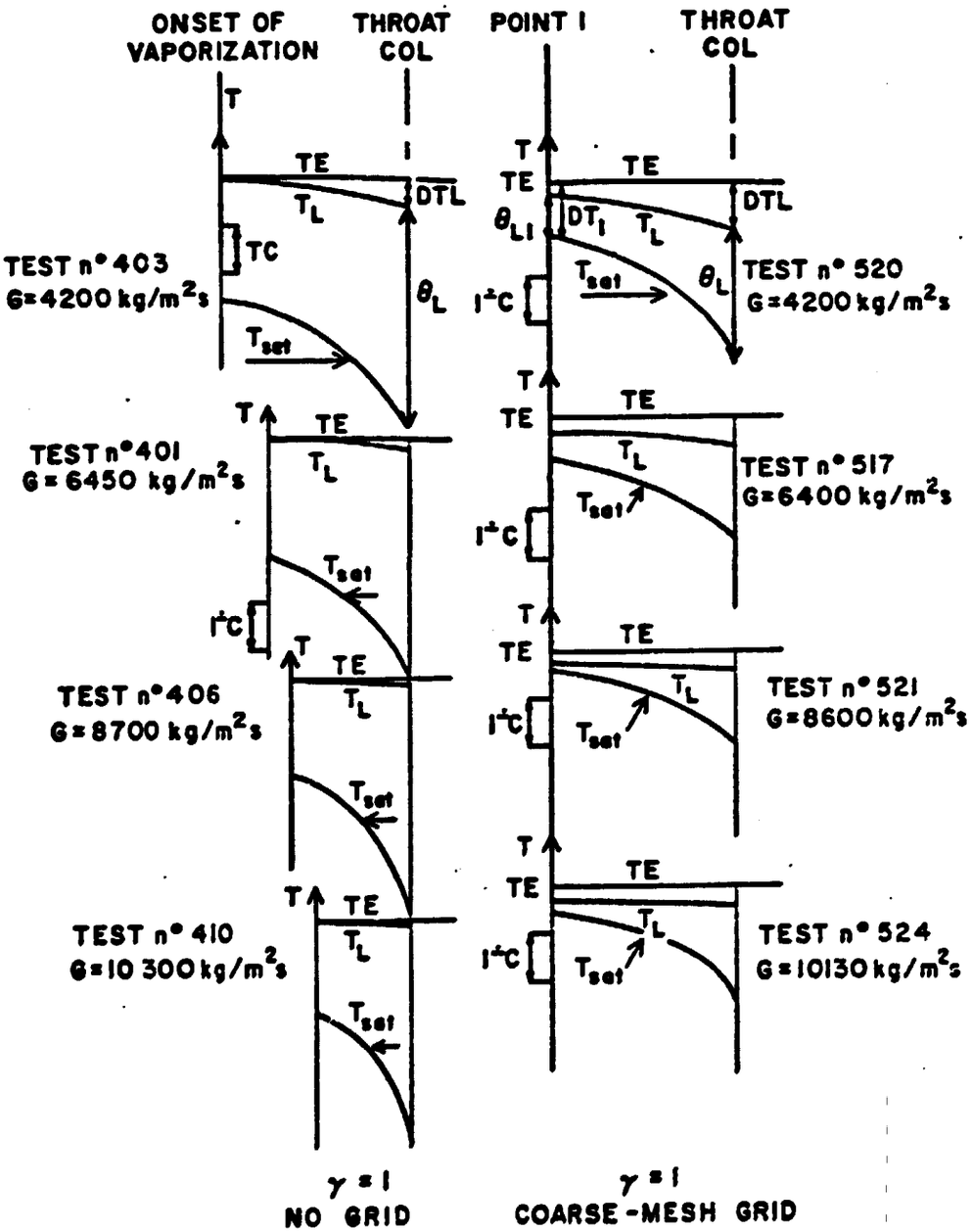

FIG. 3 - EVOLUTIONS OF THE LIQUID TEMPERATURE AND THE SATURATION TEMPERATURE

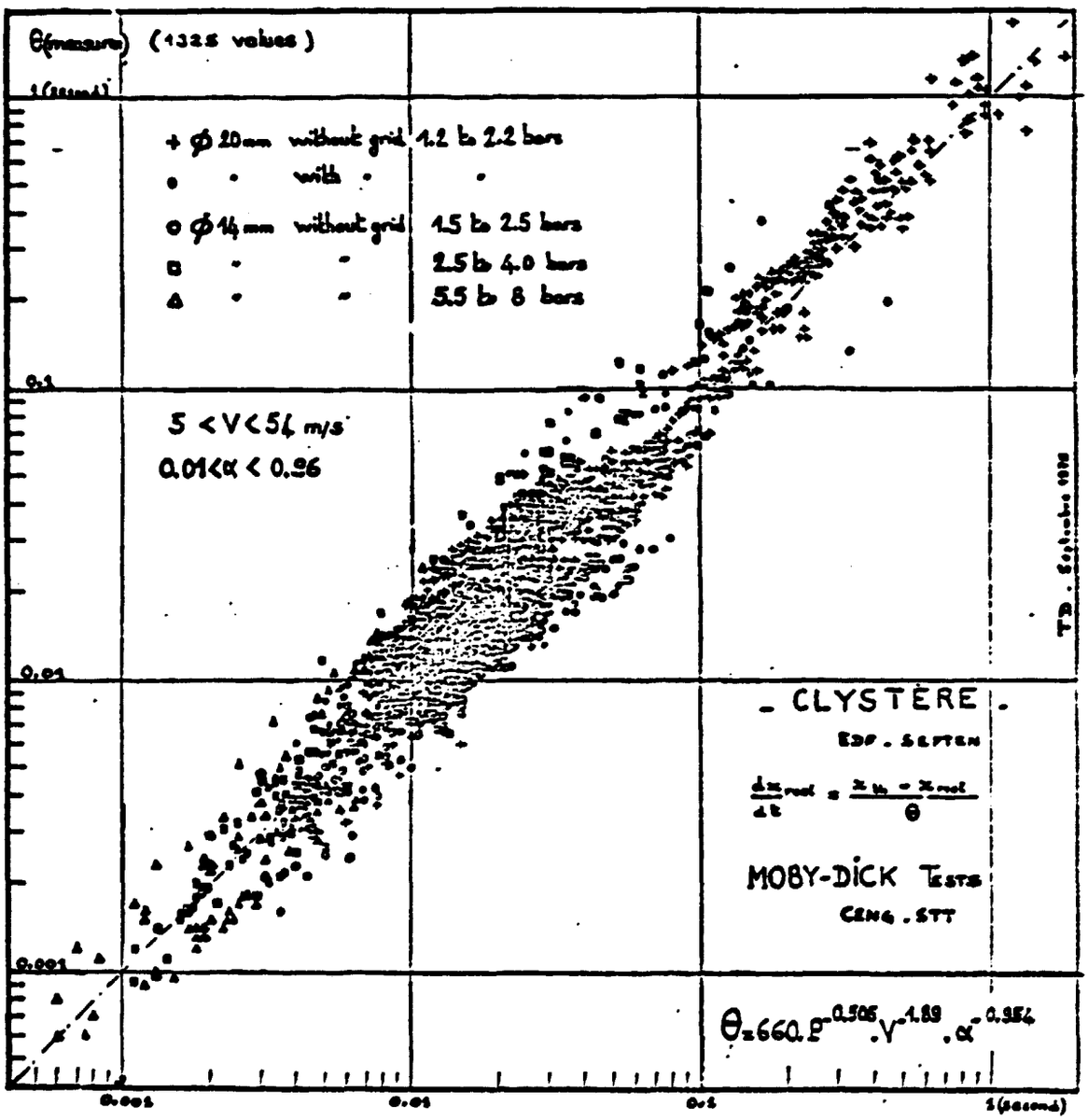

FIG. 4 - COMPARISONS OF THE MEASURED AND CORRELATED VALUES OF θ

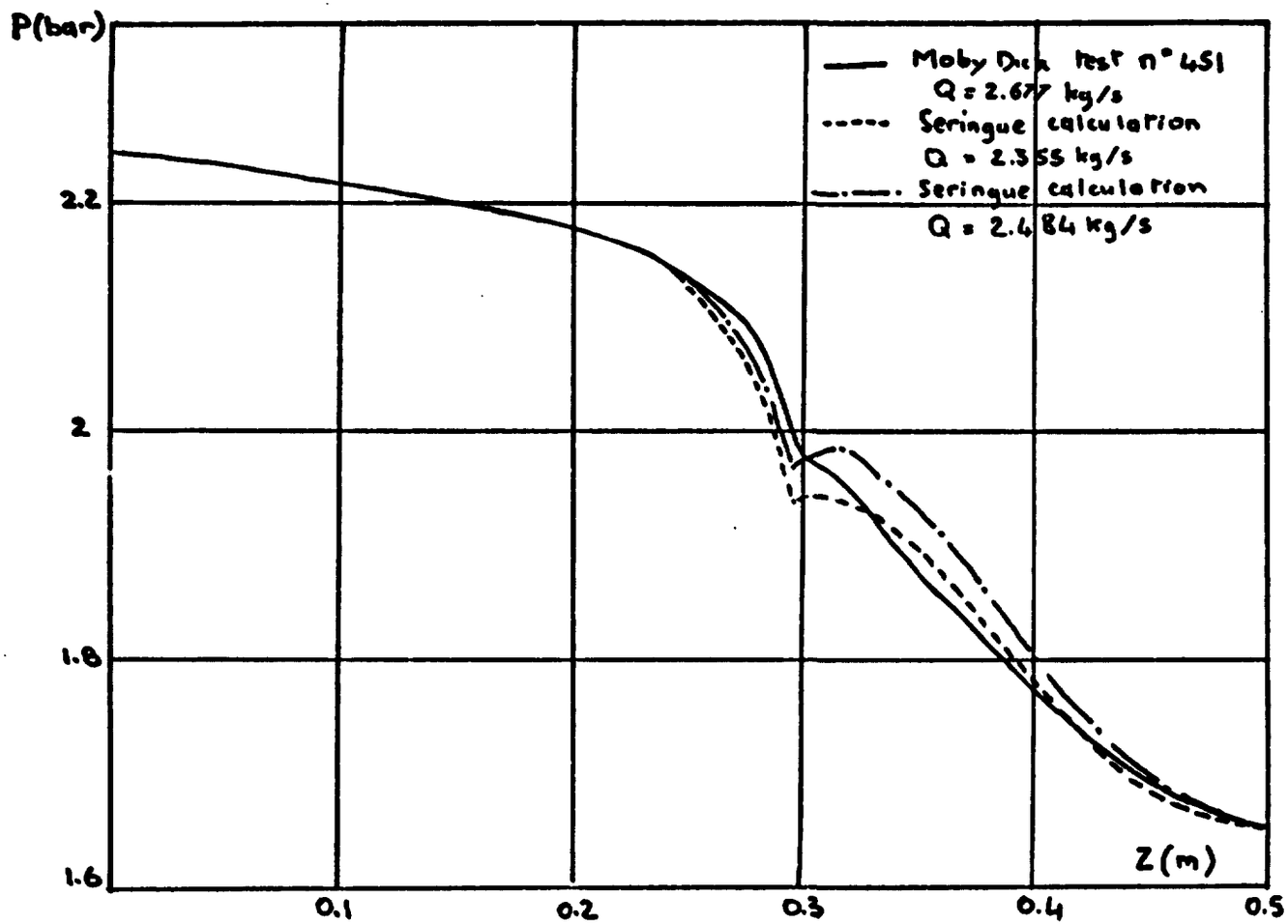

FIG. 5 - MOBY DICK STEAM-WATER TESTS : COMPARISON OF MEASURED AND CALCULATED PRESSURE LINES

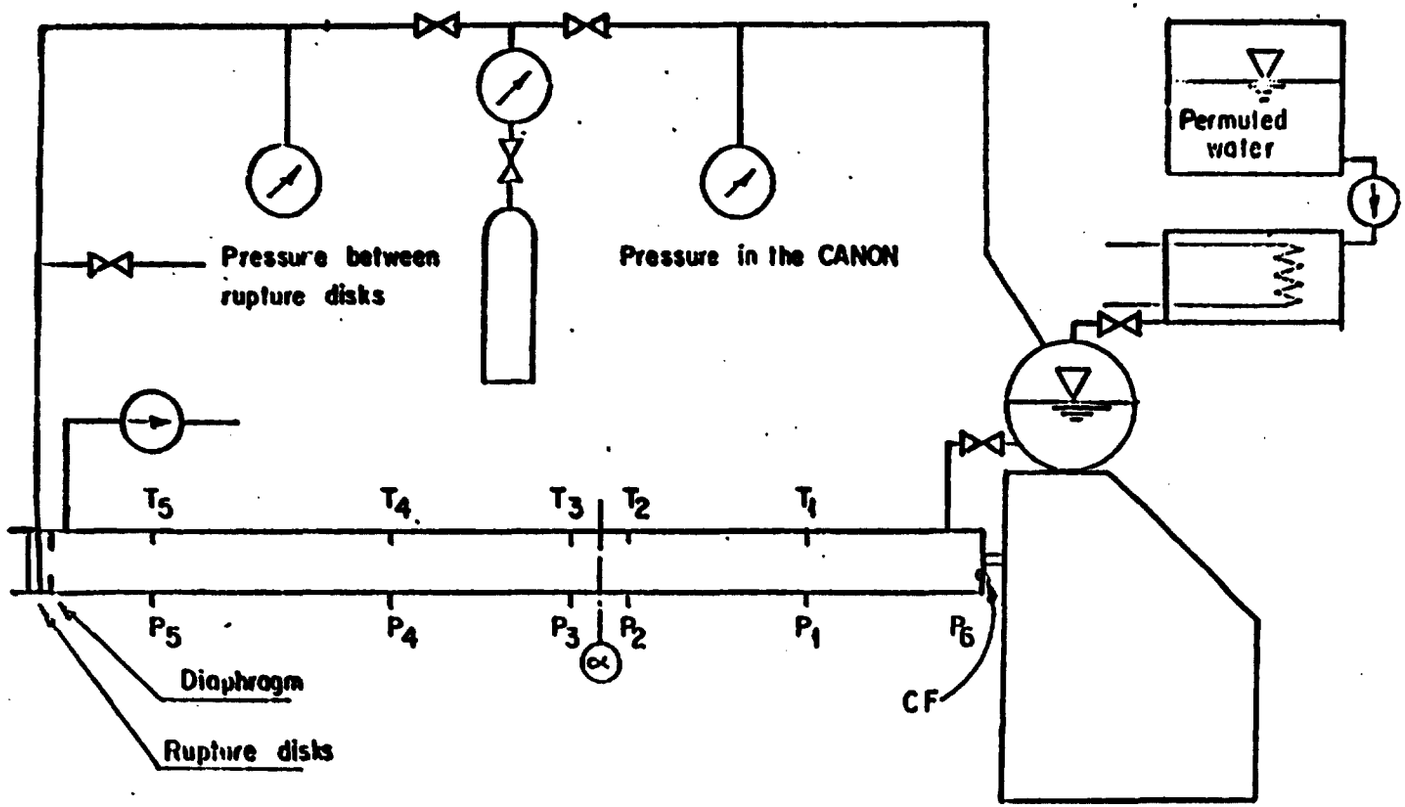

FIG. 6 - CANON APPARATUS

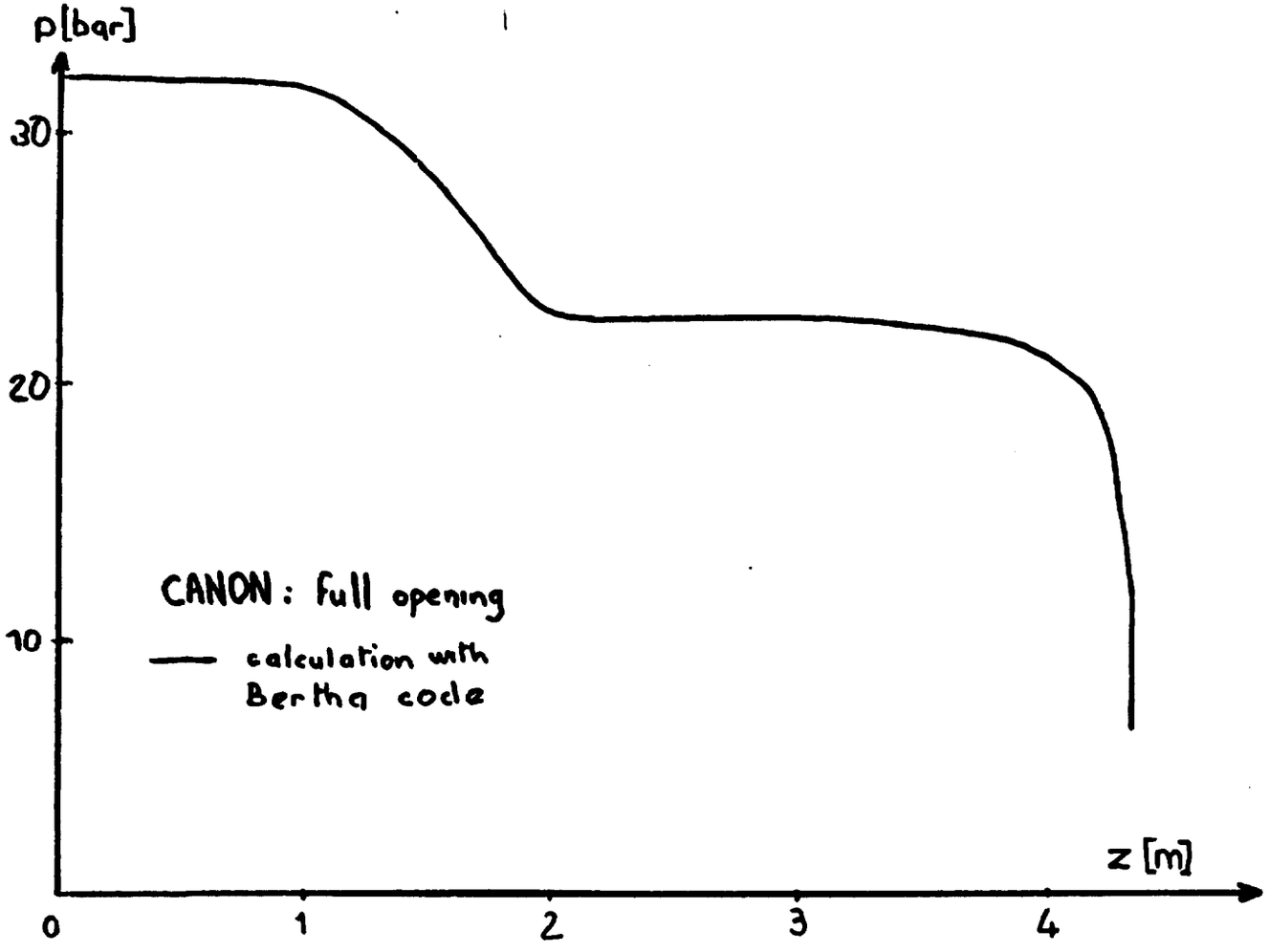

FIG. 7 - CANON TEST : PRESSURE LINE AT 3.10^{-3} SECOND

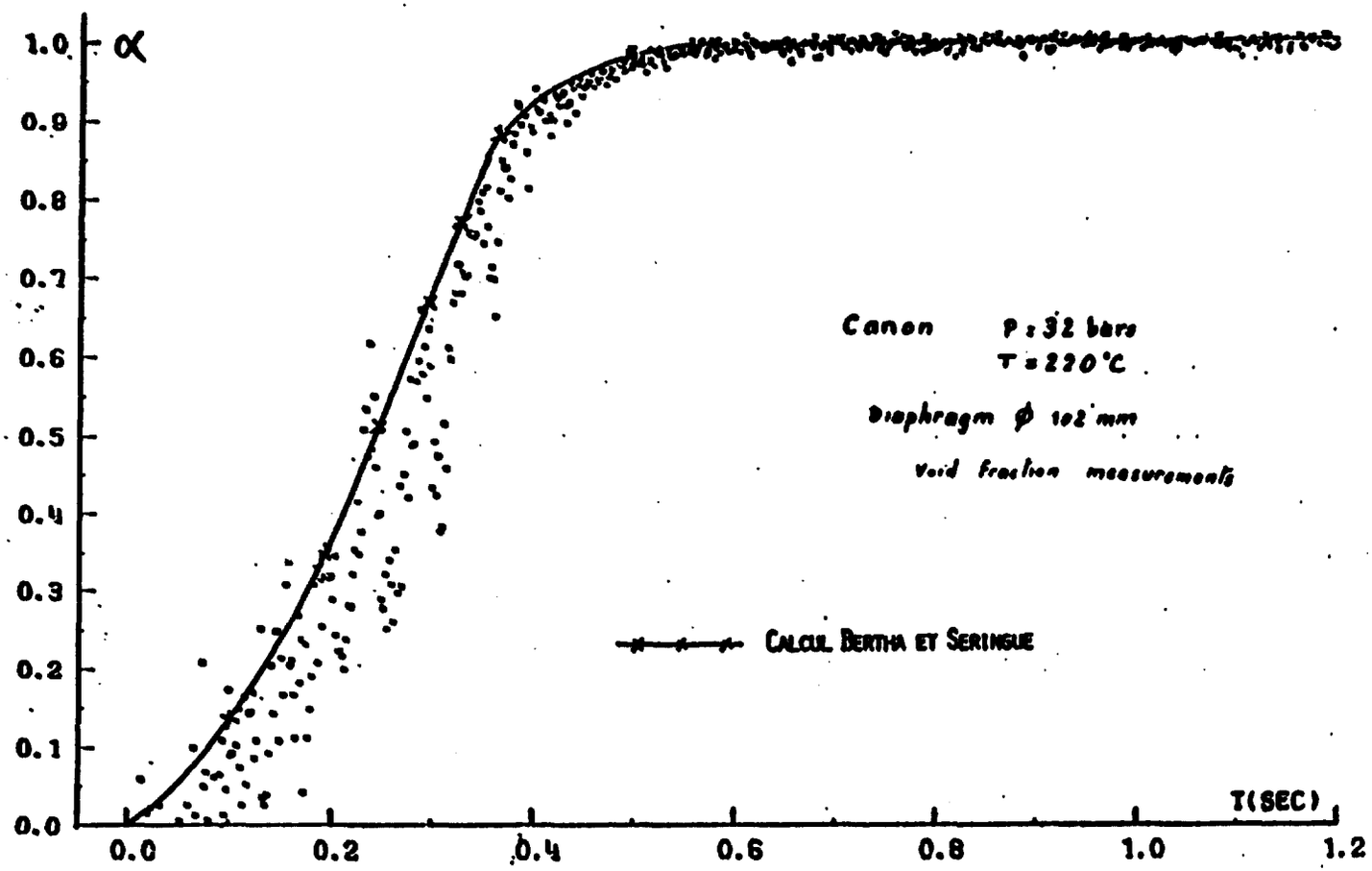

FIG. 8 - CANON TESTS : COMPARISON OF CALCULATED AND MEASURED VOID FRACTION LINES

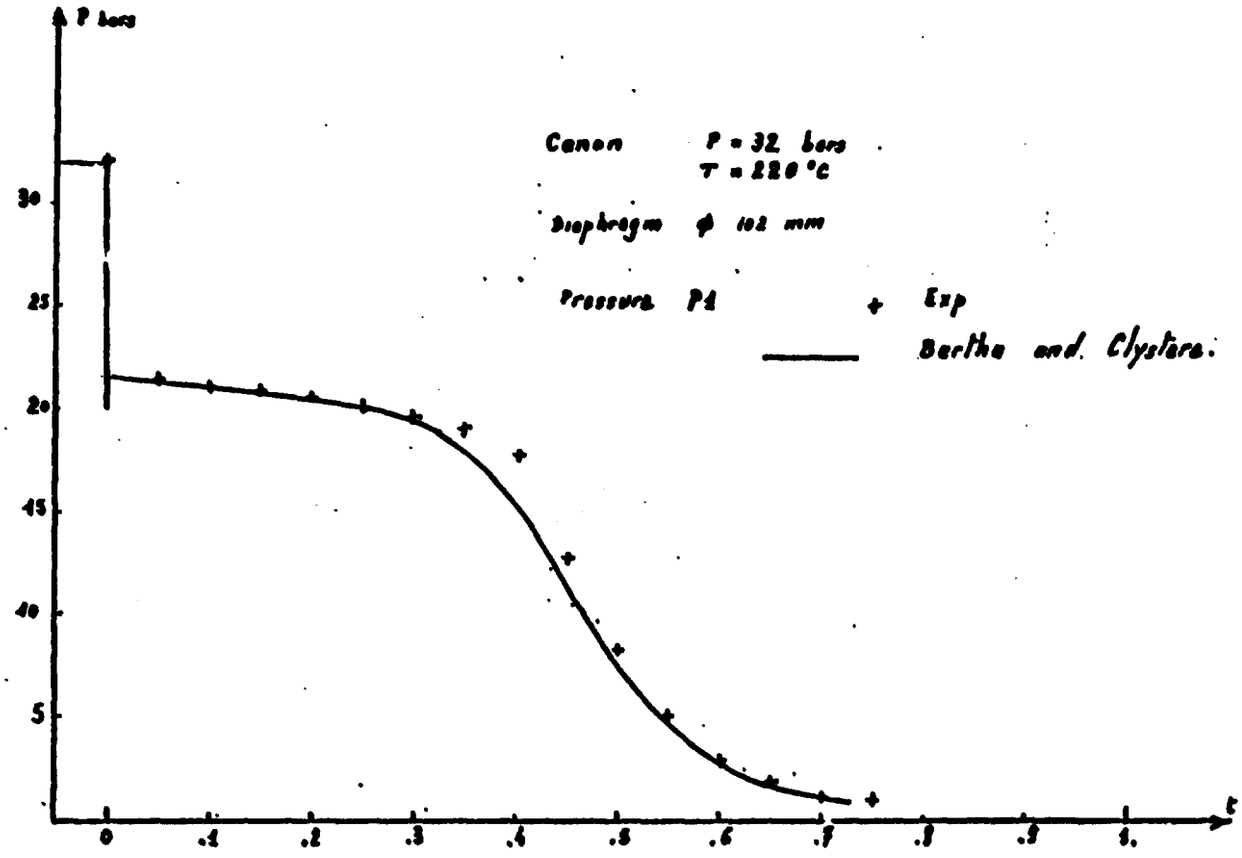

FIG. 9 - CANON TESTS : COMPARISON OF CALCULATED AND MEASURED PRESSURE LINES

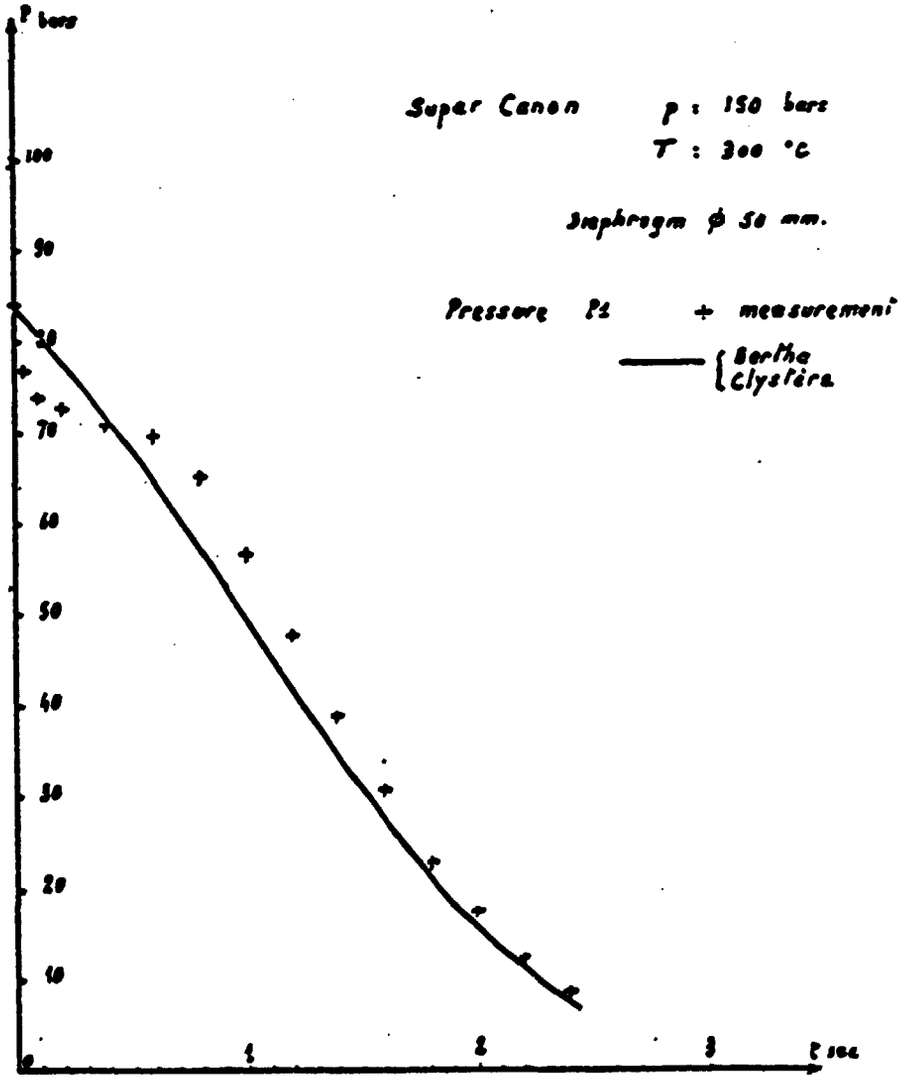

FIG. 10 - SUPER CANON TESTS : COMPARISON OF CALCULATED AND MEASURED PRESSURE LINES.

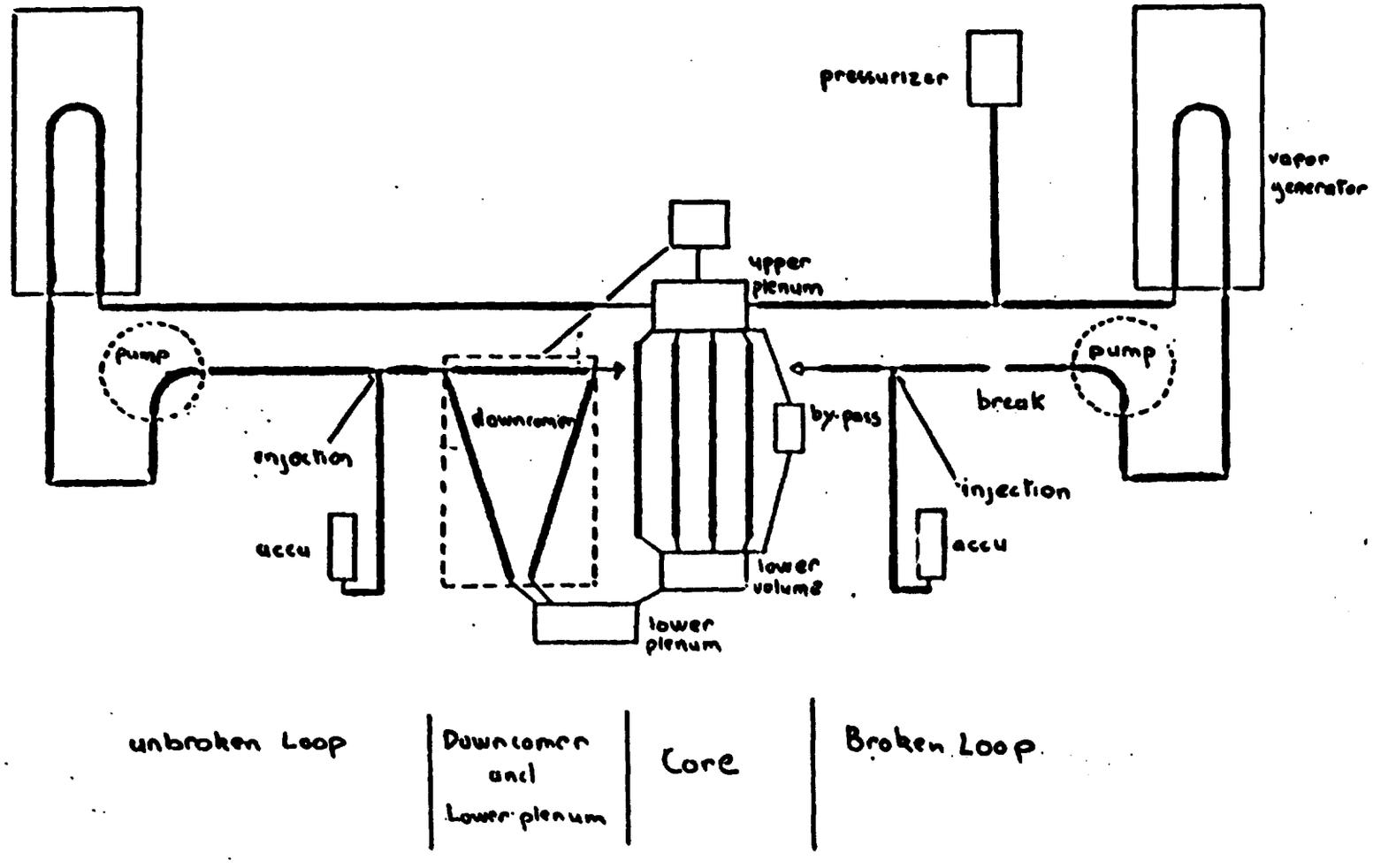

FIG. 11 - REACTOR REPRESENTATION IN CLYSTERE CODE

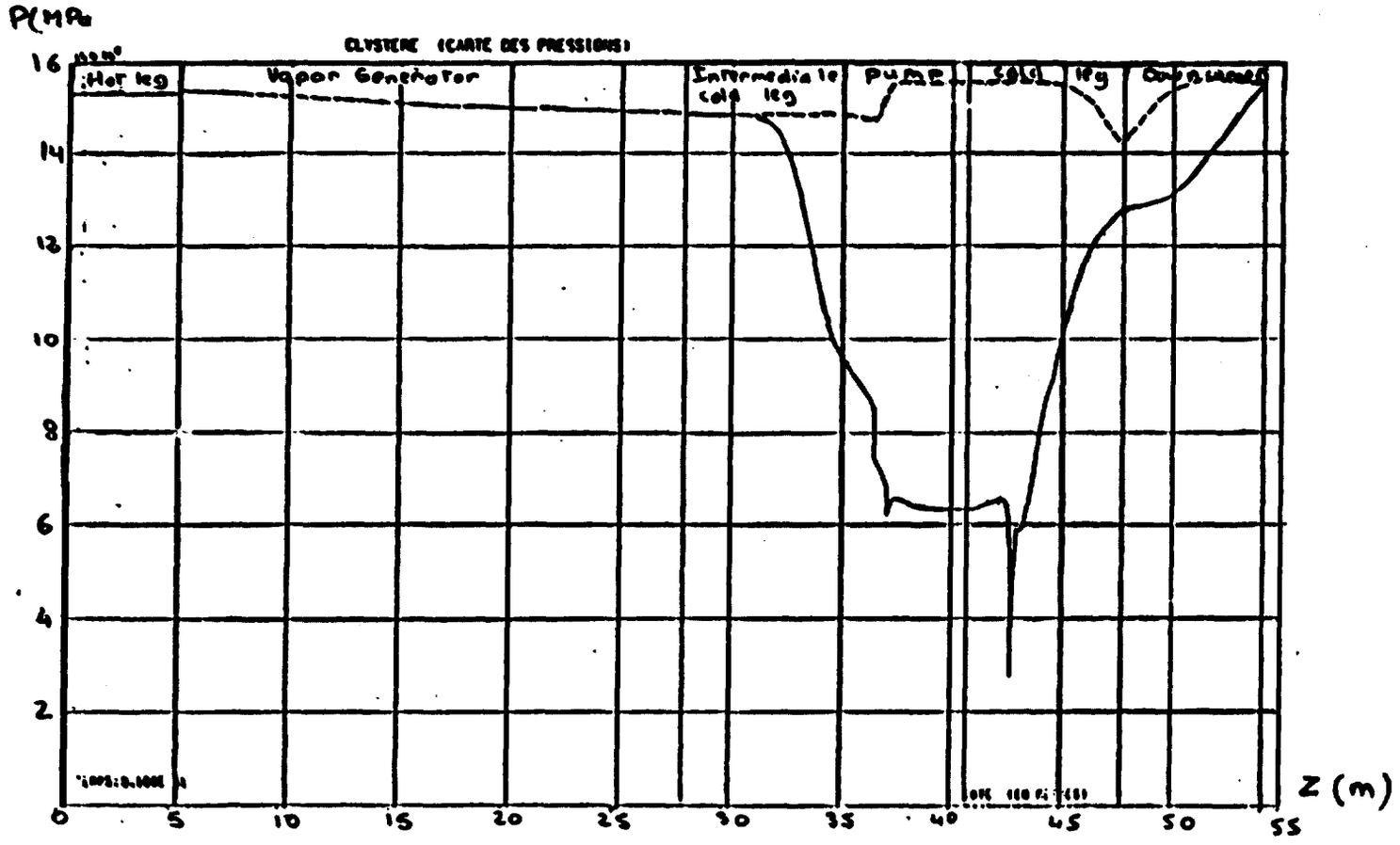

FIG. 12 : PRESSURE MAP AT 0.01 SECOND

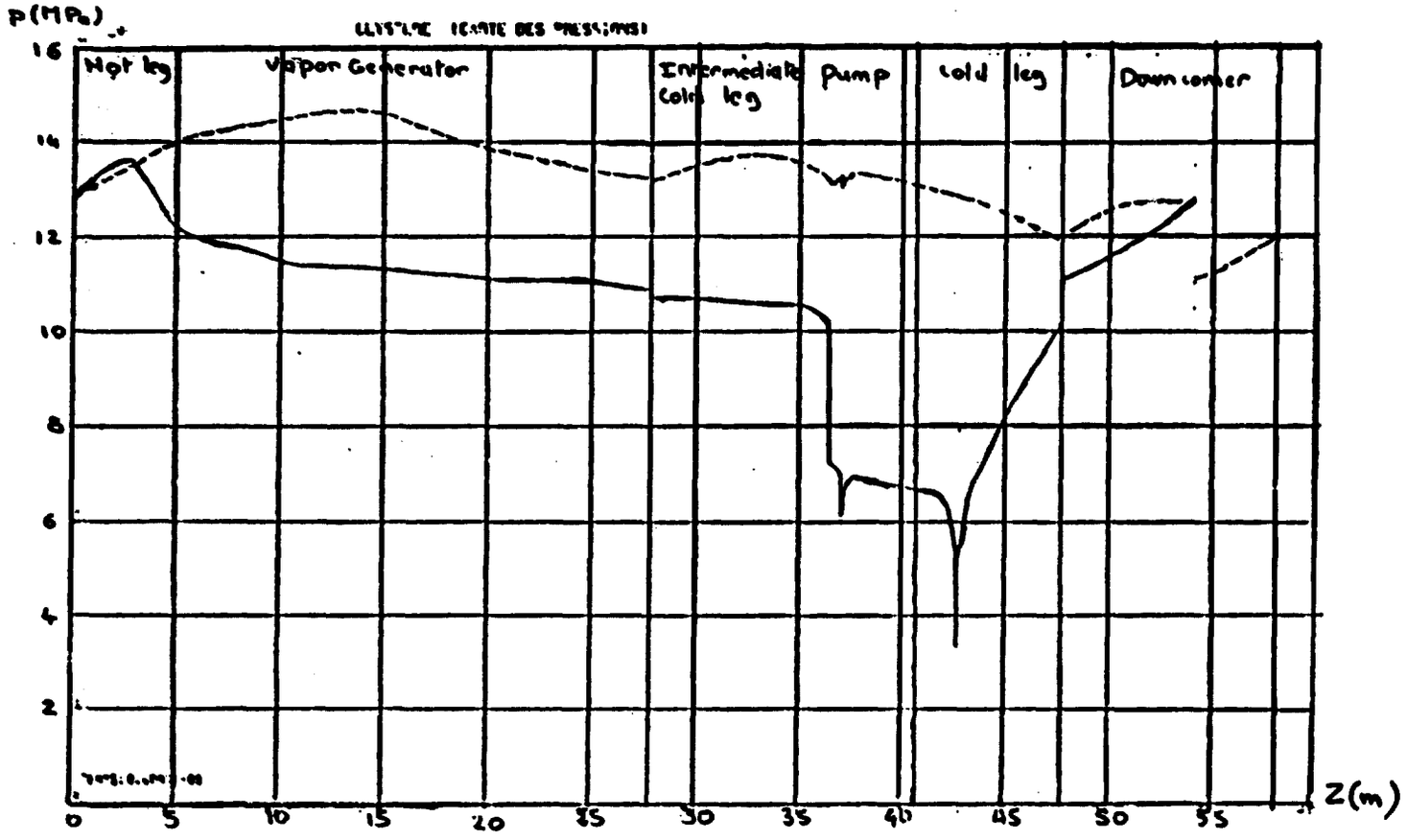

FIG. 13 - PRESSURE MAP AT 0.04 SECOND

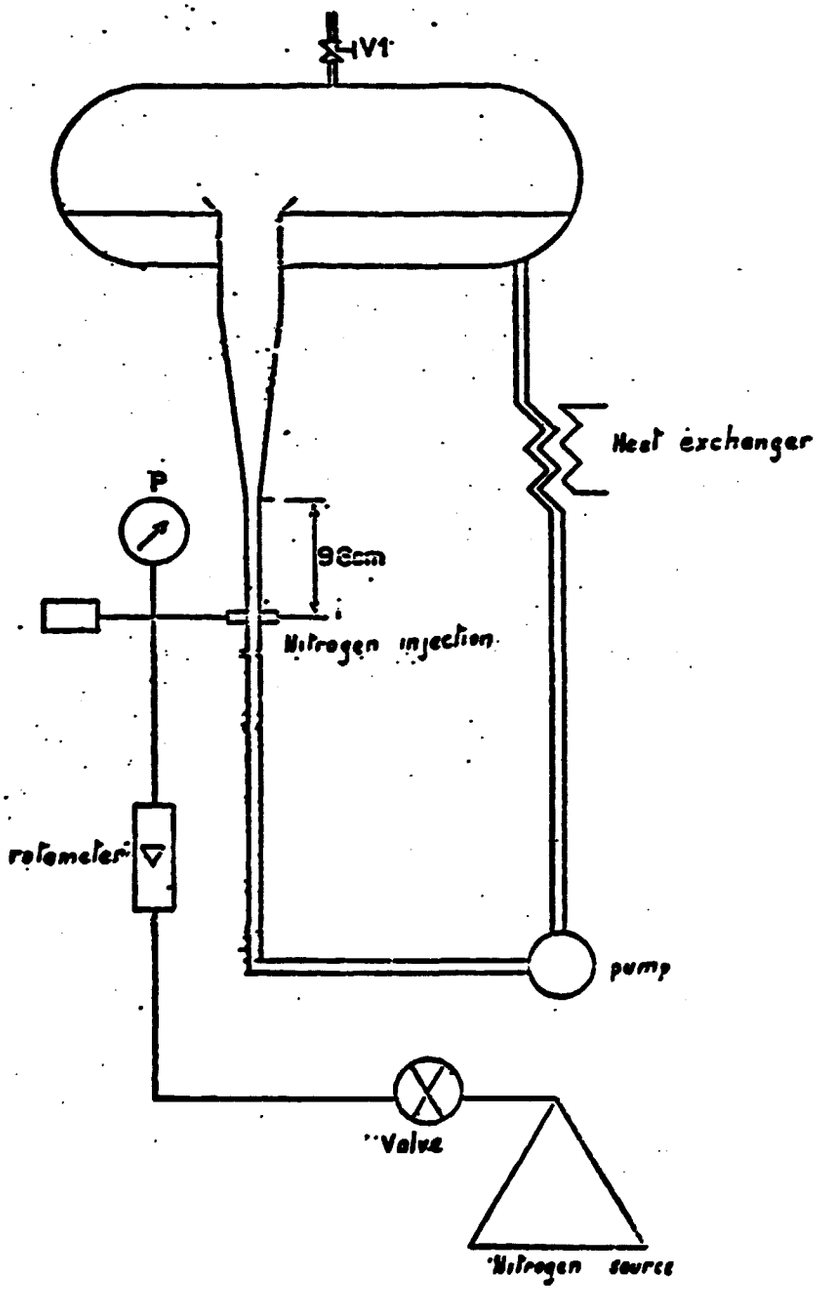

FIG. 14 - NITROGEN-WATER MOBY DICK LOOP

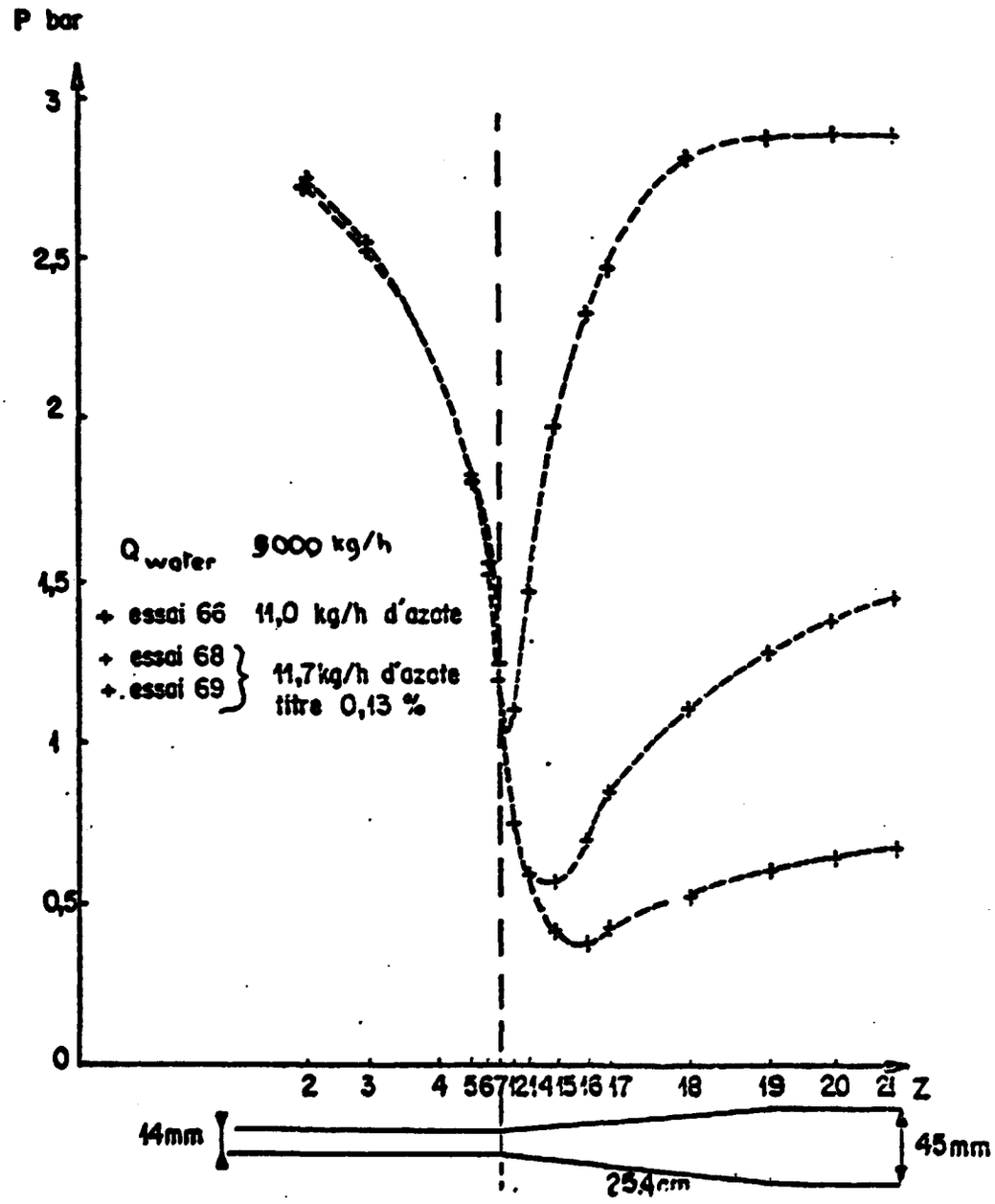

FIG. 15 - NITROGEN-WATER CRITICAL FLOW TESTS
PRESSURE LINES

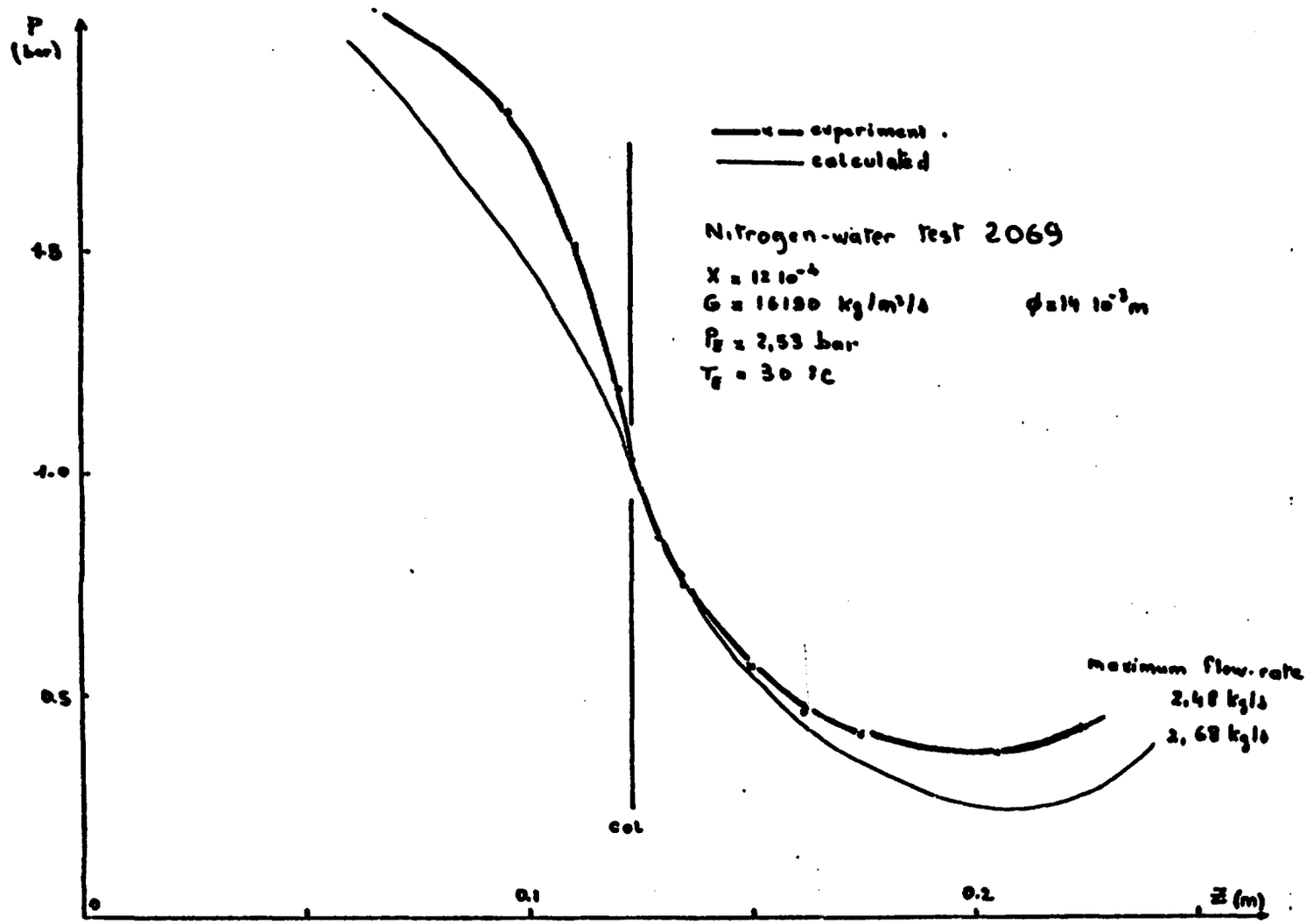

FIG. 16 NITROGEN-WATER TESTS : COMPARISON OF CALCULATED AND MEASURED PRESSURE LINES

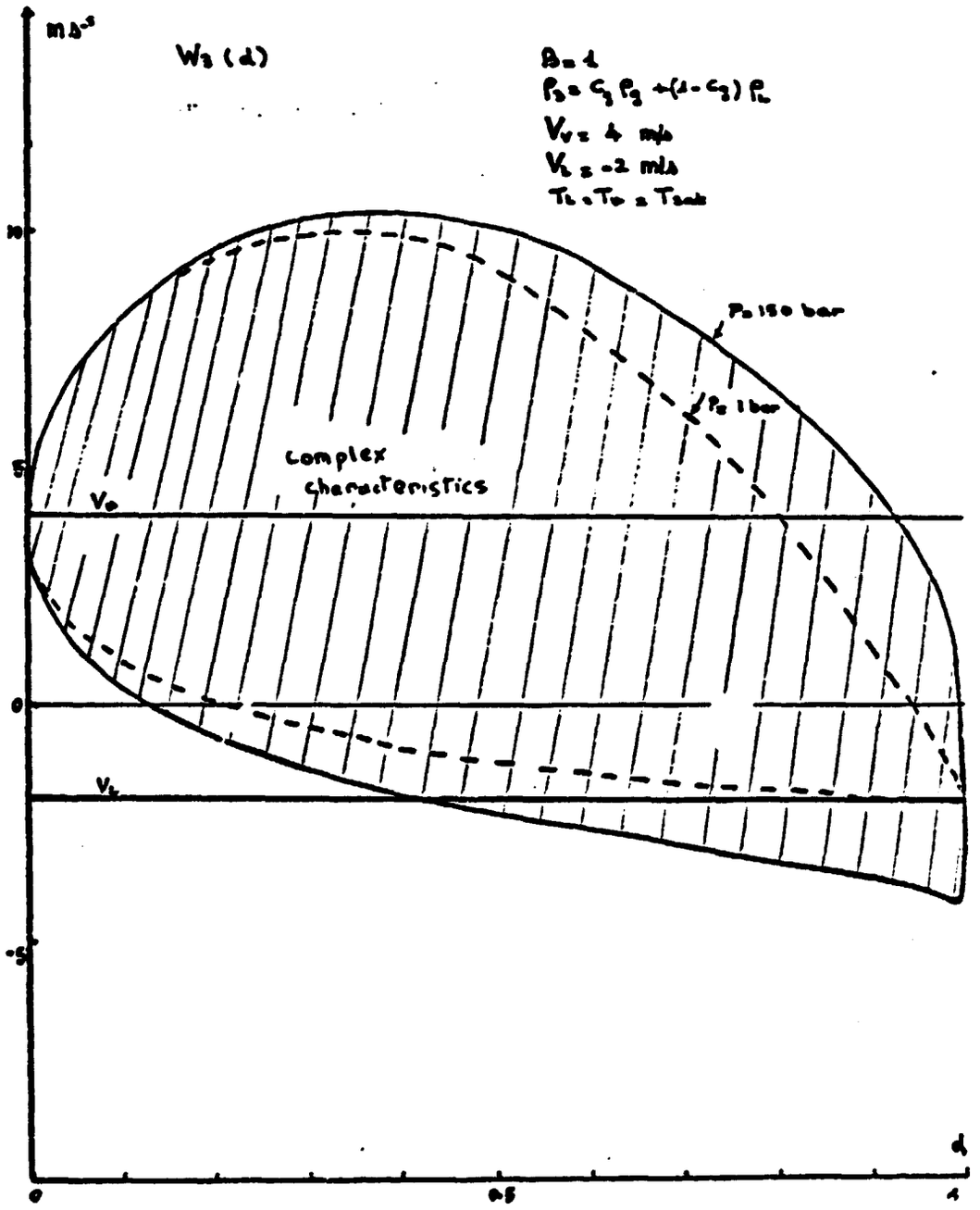

FIG. 17 - VALUES OF W_3 GIVING COMPLEX CHARACTERISTICS

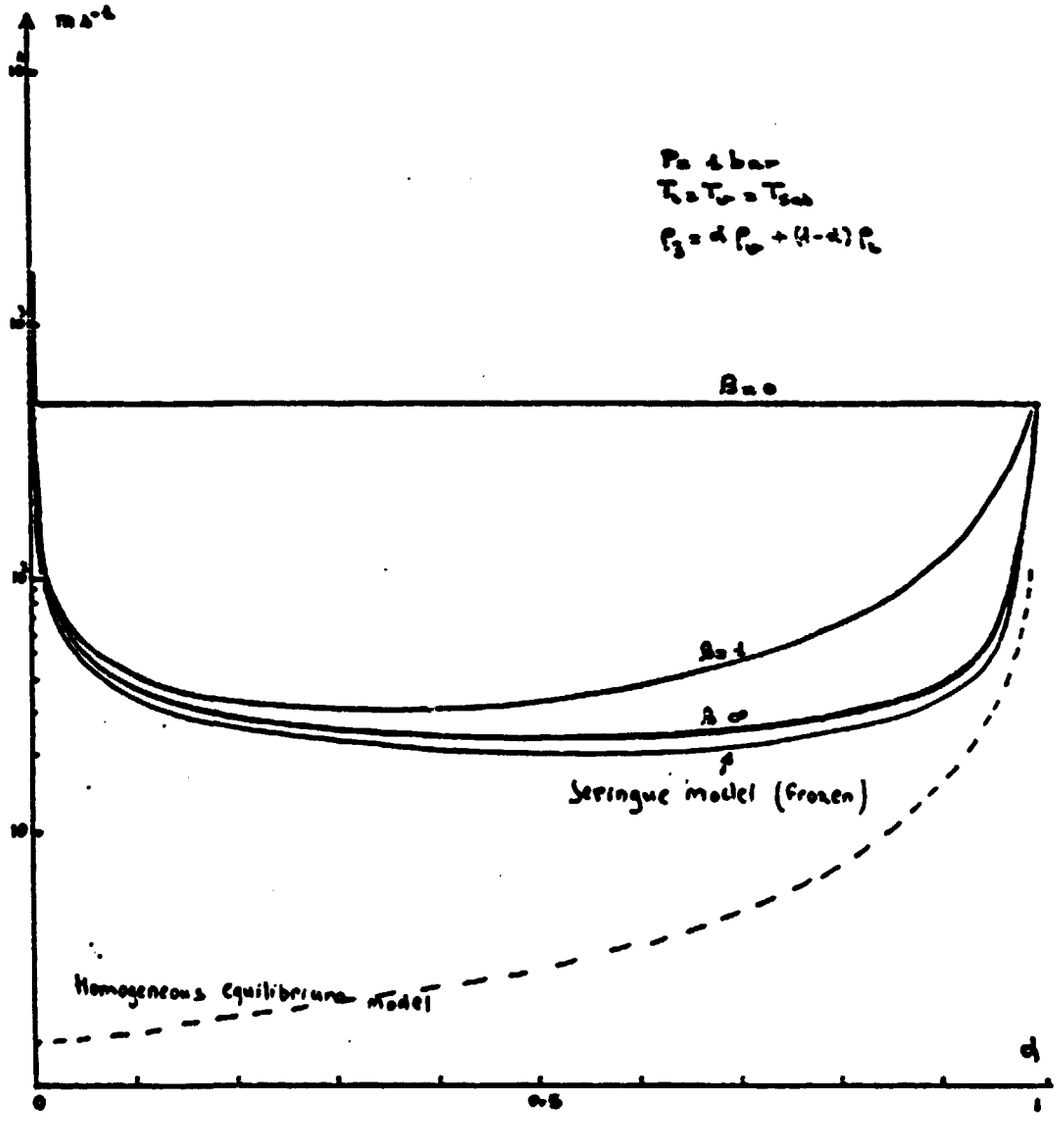

FIG. 18 - EFFECT OF INDUCED MASS TERM ON SOUND VELOCITY

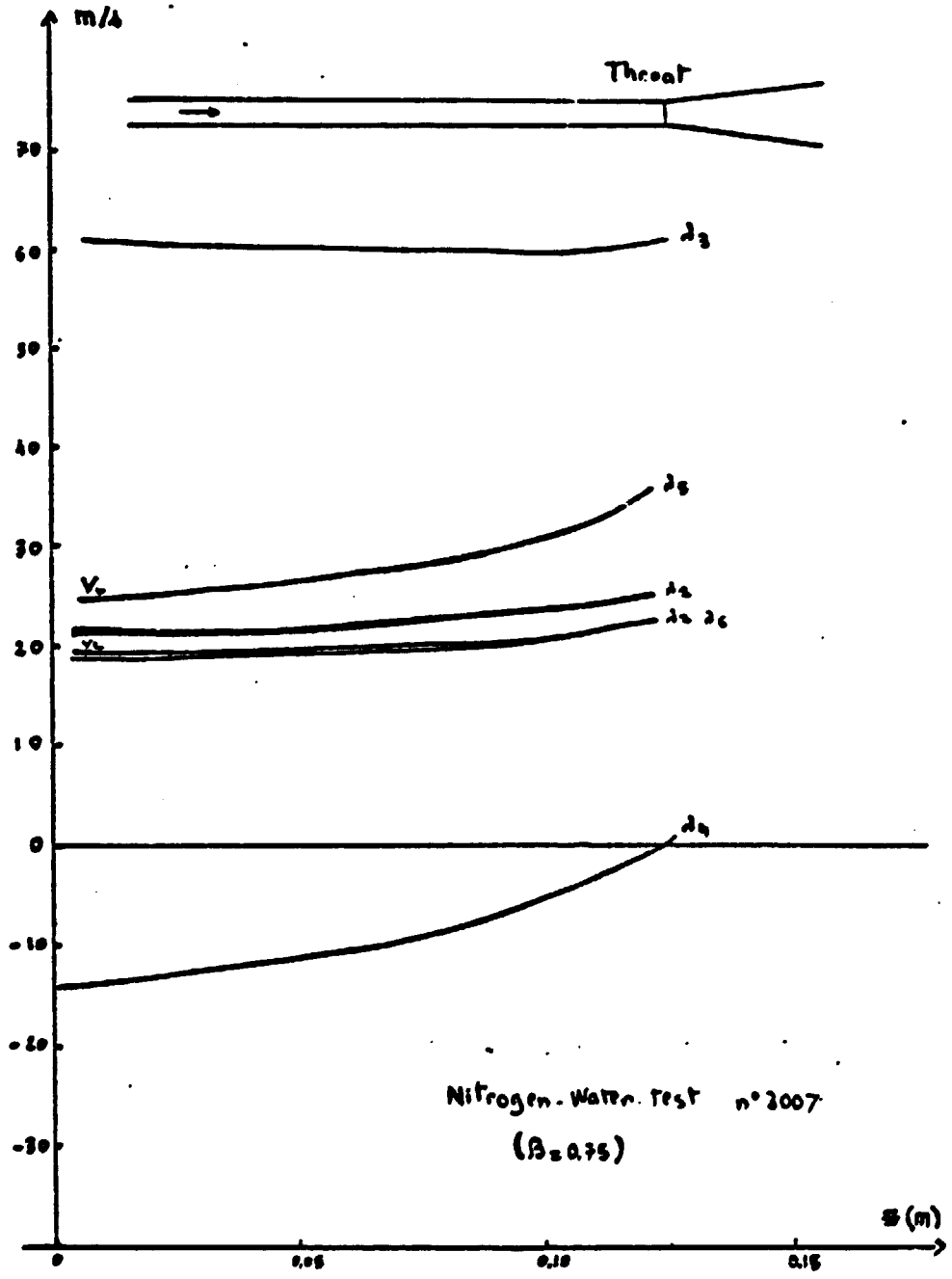

FIG. 19 - EVOLUTION OF THE CHARACTERISTIC DIRECTIONS ALONG THE FLOW